COMBUSTION AND FLAME 58: 291-300(1984)

High Temperature Kinetics of NCO

MICHEL Y. LOUGE and RONALD K. HANSON

Department of Mechanical Engineering, High Temperature Gasdynamics Laboratory, Stanford University, Stanford, CA 94305

Mixtures of cyanogen and nitrous oxide diluted in argon were shock heated to measure the ratio of the rate constants for

$$NCO + O \rightarrow CO + NO \qquad (3)$$

and

$$NCO + M \rightarrow N + CO + M. \qquad (4)$$

The diagnostic was narrow-line absorption of NCO at 440.479 nm using a remotely located cw ring dye laser source. By varying the mole fraction of nitrous oxide in the initial mixture and conducting otherwise identical experiments, we inferred at 2240°K

$$k_3/k_4 = 10^{3.54(+0.34,\,-0.37)}.$$

Utilizing a recent determination of k_3 and previous measurements of the ratio k_3/k_4, we recommend over the temperature range $2150 \leqslant T \leqslant 2400$°K

$$k_4 = 10^{16.8}T^{-0.5}\ \exp[-24000/T]\ \text{cm}^3/\text{mole/s}\ [\times 2.3,\ \times 0.4].$$

An additional mixture of cyanogen, oxygen, hydrogen, and nitrous oxide diluted in argon was shock heated and NCO was monitored to infer the rate constant for

$$NCO + H \rightarrow CO + NH \qquad (5)$$

and the ratio k_6/k_7:

$$C_2N_2 + H \rightarrow CN + HCN, \qquad (6)$$

$$CN + H_2 \rightarrow HCN + H. \qquad (7)$$

We found near 1490°K

$$k_5 = 10^{13.73(+0.42,\,-0.27)}\ \text{cm}^3/\text{mole/s},$$

and

$$k_6/k_7 = 0.81(+0.89,\ -0.47).$$

These experiments also led to an estimate of the rate constant for

$$NCO + H_2 \rightarrow HNCO + H, \qquad (8)$$

with the result, near 1490°K,

$$k_8 = 10^{12.1(+0.4,\,-0.7)}\ \text{cm}^3/\text{mole/s}.$$

Published by Elsevier Science Publishing Co., Inc.
52 Vanderbilt Avenue, New York, NY 10017

0010-2180/84/$03.00

INTRODUCTION

NCO plays an important role in the mechanism of nitric oxide formation from nitrogen-containing fuels. In an earlier paper on cyanogen oxidation kinetics [1], we utilized measurements of CN, CO, and NO to examine the formation of NCO from C_2N_2 and CN. Subsequently, we developed a novel laser absorption diagnostic of NCO [2], and we used this technique to study NCO removal in an oxidizing medium [3]. In the present study, the NCO diagnostic was used again to measure other reactions involving NCO at high temperatures.

Mixtures of C_2N_2 and N_2O diluted in argon were shock heated to measure the ratio of the rate constants of reactions (3) and (4) at 2240°K, the rate constants for the other reactions significant at early times, reactions (1) and (2), being already well established [1]:

$$N_2O + M \rightarrow N_2 + O + M, \tag{1}$$

$$C_2N_2 + O \rightarrow CN + NCO, \tag{2}$$

$$NCO + O \rightarrow CO + NO, \tag{3}$$

$$NCO + M \rightarrow N + CO + M. \tag{4}$$

Another mixture containing C_2N_2, O_2, H_2, and N_2O diluted in argon was shock heated at 1490°K to measure the rate constant of

$$NCO + H \rightarrow CO + NH, \tag{5}$$

and the ratio k_6/k_7:

$$C_2N_2 + H \rightarrow CN + HCN, \tag{6}$$

$$CN + H_2 \rightarrow H + HCN. \tag{7}$$

In addition this mixture led to an estimate for the rate constant of

$$NCO + H_2 \rightarrow HNCO + H. \tag{8}$$

Previous work to establish k_3 and k_4 is limited primarily to our own shock tube work in which we determined the ratio k_3/k_4 at 2150 and 2400°K from measurements of NO and CN [1], and k_3 by monitoring NCO using laser absorption [3]. There are no previous data for k_5 and k_8; the limited data for k_6 and k_7 have been reviewed by Baulch et al. [4]. In addition, we note the recent shock tube work in our laboratory by Szekely, Hanson, and Bowman, who measured k_7 in the range $2700 \leqslant T \leqslant 3500°K$ [5], and the reverse rate of reaction (6) in the range $2720 \leqslant T \leqslant 3070°K$ [6].

In this paper, the experimental facility and optical technique will be briefly described; then the data reduction and results for each of the mixtures will be presented.

EXPERIMENTAL

The experiments were conducted in a 15.24 cm internal diameter stainless-steel pressure-driven shock tube [7]. Shock speeds varied between 1.2 and 1.5 mm/μs with attenuation of 0.3%/m or less. Typical leak plus outgassing rates were 3-5 $\times 10^{-5}$ Torr/min. Gases were taken directly from commercial cylinders (Matheson) with the following purities: O_2, H_2,and N_2O (>99.9%); C_2N_2 (1.01% diluted in argon; HCN and CNCl < 50 ppmv, O_2 < 20 ppmv, CO_2 < 20 ppmv). The shock tube test section and laser absorption system for NCO are shown schematically in Fig. 1. The absorption from the $P_2 + {}^PQ_{12}$ band head of the $[A^2\Sigma^+(00^00) \leftarrow X^2\Pi_i(00^10)]$ band of NCO at 440.479 nm (vac.) was used to monitor NCO. This system was described in detail elsewhere [3]. It consisted of an Ar^+-pumped ring dye laser with a typical output power of 60 mW (single-mode) at 440.5 nm. After amplitude stabilization, the output was transported 65 m via a 200 μm optical fiber to the shock tube facility, where it was double-passed through the shock tube test section. The incident and return beams were filtered (FWHM: 40 nm, center at 450 nm) and monitored on separate detectors. The signals were electronically balanced prior to each experiment using small dc offset and gain adjustments on one of the differential amplifiers. The difference $(i_0 - i)$ and reference (i_0) signals were recorded on two separate channels of a digital oscilloscope (Nicolet Explorer III, dc-coupled through a 100 kHz upper frequency cutoff filter). The data were subsequently transferred to a computer for analysis.

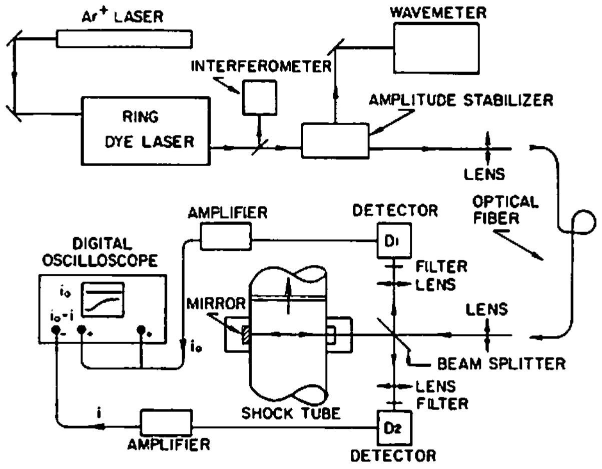

Fig. 1. Shock tube NCO laser absorption diagnostic at 440.479 nm.

Six runs were conducted behind incident shock waves with the following mixtures and conditions: $\chi_{C_2N_2} \simeq 0.41\%$, $0.10 \leqslant \chi_{N_2O} \leqslant 0.42\%$, $T_2 \simeq 2240$°K, $p_2 \simeq 0.65$ atm, and $\rho_{21} \simeq 3.57$. (ρ_{21} is the density ratio across the shock and also the ratio of particle time to laboratory time.) The temperature of the experiments was set by considerations of growing interferences on the NCO absorption system from spontaneous emission at higher temperatures and by insufficient rates of NCO removal from reaction (4) at lower temperatures:

$$NCO + M \rightarrow N + CO + M. \tag{4}$$

An additional mixture of H_2, O_2, N_2O, C_2N_2, and argon was shock heated with $\chi_{H_2} \simeq 0.58\%$, $\chi_{O_2} \simeq 0.09\%$, $\chi_{N_2O} \simeq 0.41\%$, $\chi_{C_2N_2} \simeq 0.40\%$, $T_2 \simeq 1490$°K, $p_2 \simeq 0.63$ atm, and $\rho_{21} \simeq 3.34$. Here, the temperature was set by considerations of growing interferences on NCO removal by reaction (4) at higher temperatures and diminishing confidence in the rate of reaction (1) at lower temperatures. Vibrational equilibrium of NCO was assumed in all experiments [3].

The transimssion of the laser system is related to the level of NCO through the Lambert-Beer law,

$$i/i_0 = \exp[-\beta(T)p_{NCO}L],$$

where i/i_0 is the fractional transmission, $\beta(T)$ is the absorption coefficient at 440.479 nm and the temperature T, p_{NCO} is the partial pressure of NCO, and L is the path length (30.5 cm). $\beta(T)$ has been experimentally determined in our laboratory at 1450°K [2] and can be extrapolated to other temperatures using a spectroscopic model [2].

$N_2O/C_2N_2/Ar$ MIXTURES-ANALYSIS AND RESULTS

a. Simplified Reaction Mechanism

A complete mechanism that encompasses 17 reactions in the C/N/O system was used in the data reduction (see Table 1), but a simplified description, useful in guiding the actual data interpretation, can be given as follows. N_2O decomposes exponentially to provide O-atoms, which rapidly reach a steady-state concentration; C_2N_2 then reacts to form NCO, which in turn is removed either by O-atoms or by dissociation:

$$N_2O + M \rightarrow N_2 + O + M, \tag{1}$$

$$C_2N_2 + O \rightarrow NCO + CN, \tag{2}$$

$$NCO + O \rightarrow CO + NO, \tag{3}$$

$$NCO + M \rightarrow N + CO + M. \tag{4}$$

TABLE 1
Reaction Mechanism—$N_2O/C_2N_2/Ar$ Mixtures

	Reaction	ΔH[a]	Equilibrium Constant[b]	Rate Constant[c] $\log_{10} A$	m	θ(°K)	Reference
1	$N_2O + M \rightarrow N_2 + O + M$	+40	−2.1	23.89	−2.5	32,710	[16]
2	$C_2N_2 + O \rightarrow CN + NCO$	+3	0.5	12.66	0	4440	[1]
3	$NCO + O \rightarrow CO + NO$	−106	10.5	13.75	0	0	[3]
4	$NCO + M \rightarrow N + CO + M$	+48	−3.7	16.80	−0.5	24,000	This study
9	$CN + O_2 \rightarrow NCO + O$	−1	0.1	12.75	0	0	[1]
10	$CN + O \rightarrow CO + N$	−75	6.7	13.31	0	210	[1]
11	$N_2O + O \rightarrow NO + NO$	−39	5.3	13.84	0	13,400	[16]
12	$N_2O + O \rightarrow N_2 + O_2$	−83	8.3	14.00	0	14,100	[16]
13	$N_2 + O \rightarrow N + NO$	+75	−6.8	14.26	0	38,370	[16]
14	$NO + O \rightarrow N + O_2$	+32	−3.8	9.58	1.0	20,820	[16]
15	$NCO + N \rightarrow N_2 + CO$	−182	17.3	13.30	0	0	[18]
16	$NCO + N \rightarrow CN + NO$	−31	3.7	14.66	0	5530	[19][d]
32	$NCO + C \rightarrow CN + CO$	−137	13.3	14.00	0	0	estimate
33	$CN + N \rightarrow C + N_2$	−44	4.0	14.64	0	4530	[20]
34	$N_2O + CN \rightarrow NCN + NO$	+4	0.8	4.60	2.5	6080	[21]
35	$NCN + O \rightarrow CN + NO$	−43	4.5	10.20	1.1	1160	[21]
36	$NCN + N \rightarrow CN + N_2$	−119	11.3	10.50	0.9	0	[21]
37	$C_2N_2 + M \rightarrow CN + CN + M$	+126	−10.0	34.46	−4.5	63,150	[17]

[a] Heat of reaction at 2200°K (kcal/mole) [10]. Thermochemical data were taken from the JANAF tables for all species [10], except for CN, where we used $\Delta Hf_0°$ (CN) = 101.2 kcal/mole, an average of the values of JANAF [10] and Colket [27].

[b] $\log_{10}(k_{\text{forward}}/k_{\text{backward}})$ at 2200°K [10].

[c] Using the notation $k = AT^m \exp[-\theta/T]$ (cm³/mole/s).

[d] Colket measured $k_{\text{backward}} = 10^{14} \exp[-21190/T]$ (cm³/mole/s); we assumed $k_f/k_b = 4.54 \exp[15660/T]$.

At the peak of the NCO concentration, we have

$$\frac{d[NCO]}{dt} \simeq k_2[C_2N_2][O] - k_3[NCO][O] - k_4[NCO][M] = 0,$$

and hence

$$\frac{[C_2N_2]}{[NCO]^{\text{peak}}} \simeq \frac{k_3}{k_2} + \frac{k_4}{k_2} \times \frac{[M]}{[O]} .$$

The mole fraction of O-atoms at steady-state is proportional to the initial N_2O mole fraction, and we have $[O]/[M] \propto (\chi_{N_2O})_{t=0}$. If $[C_2N_2]$ is nearly constant throughout the time scale of interest, measurements of the peak NCO concentration for different values of the initial N_2O mole fraction can be plotted as a straight line on a graph showing $[C_2N_2]/[NCO]^{\text{peak}}$ as a function of $1/(\chi_{N_2O})_{t=0}$. In the case of this simple model, the intercept and the slope are proportional to, respectively, the ratios k_3/k_2 and k_4/k_2. Furthermore, the ratio of the intercept and the slope yields k_3/k_4.

b. Results and Discussion

A numerical routine derived from the NASA-Lewis general chemical kinetics program [8], and incorporating the mechanism in Table 1, was used for the actual data interpretation. Thermochemical data were taken from the JANAF tables for all species [10], except for

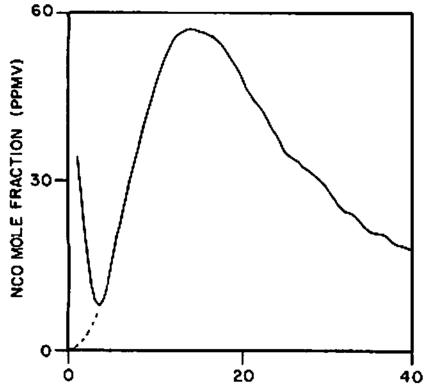

Fig. 2. A typical experimental trace in $N_2O/C_2N_2/Ar$ mixtures with $T_2 = 2210°K$, $p_2 = 0.64$ atm, $N_2O : C_2N_2 : Ar = 2 : 4 : 994$, *and* $\rho_{21} = 3.56$. The initial spike corresponds to a shock-generated Schlieren effect. The dashed line is an estimate of the unperturbed NCO profile at early times. The peak absorption of 1.9% corresponds to $X_{NCO} \simeq 57$ ppmv, with $\beta(2210°K) \simeq 17\ cm^{-1}\ atm^{-1}$ [2].

CN, where we used $\Delta Hf_0^{\circ} = 101.2$ kcal/mole, an average of the values of JANAF [10] and Colket [27]. Figure 2 shows a typical experimental trace, converted to NCO mole fraction. The initial spike results from a Schlieren effect, which is useful in determining the shock arrival time. The NCO mole fraction at the peak ($t \simeq 14 \mu s$) was used in the data reduction. Values for k_3/k_2 and k_4/k_2 were inferred by varying these quantities in the detailed kinetic mechanism until least-squares agreement was found between the experimental and computer-generated results for $[C_2N_2]/[NCO]^{peak}$ versus $1/(\chi_{N_2O})_{t=0}$ (see Fig. 3). Finally, the ratio k_3/k_4 was computed from the ratio of the inferred values of k_3/k_2 and k_4/k_2.

Computer calculations confirmed that the ratio k_3/k_4 inferred by this procedure is reasonably insensitive to the value of k_2 employed in the detailed model (see Fig. 3); hence the value k_3/k_4 reported is nearly independent of the substantial uncertainties associated with both k_2 [1] and the absorption coefficient $\beta(T = 2240°K)$ [2]. Residual uncertainties in k_3/k_4 result primarily from the uncertain knowledge of other rate constants in the mechanism [×1.7, ×0.6], and the 95% confidence interval on the fit to the data in Fig. 3 [×1.8, ×0.5] [9]. These two uncorrelated uncertainties can be combined to give an overall uncertainty in k_3/k_4 of [×2.2, ×0.43], which means that the ratio k_3/k_4 is bounded by values 2.2 times and 0.43 times the reported value. No significant uncertainty in k_3/k_4 resulted from uncertain heats of reaction (e.g., for CN or NCO) since most reactions proceeded in the forward direction. Figure 4 shows computer-generated profiles of reactants and intermediate species using the values of k_3/k_2 and k_4/k_2 inferred from Fig. 3 and other rates reported in the detailed mechanism of Table 1.

Our result $k_3/k_4 = 10^{3.54(+0.34,-0.37)}$ at 2240°K is plotted in Arrhenius form along with our earlier determinations at 2150 and 2400°K (Fig. 5), which were obtained in two independent experiments based on measurements of NO and CN [1]. Reasonable agreement is found among the three independent measurements within the size of their individual error bars. Because of these error bars and the narrow range of temperatures studied, it is difficult to estimate a correct temperature dependence of the ratio. For the purpose of reporting a single expression,

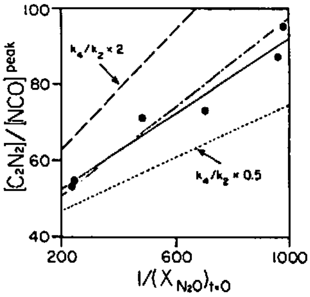

Fig. 3. Experimental plot of the concentrations ratio $[C_2N_2]/[NCO]^{peak}$ versus inverse initial N_2O mole fraction $1/(\chi_{N_2O})_{t=0}$ with $T_2 \simeq 2240°K$ and $p_2 \simeq 0.65$ atm. The peak NCO concentrations were computed using absorption coefficients from Louge et al. [2]. The solid line is a least-squares fit to the experimental data and also a best computer correlation using the mechanism in Table 1, $k_3/k_2 = 10^{1.38}$ and $k_4/k_2 = 10^{-2.16}$. The dashed line corresponds to $k_4/k_2 \times 2$ and the dotted line to $k_4/k_2 \times 0.5$ (with k_2 held at the Table 1 value). Clearly, neither excursions in k_4/k_2 can adequately fit the experimental slope. The dot-dash line shows insensitivity to the nominal value of k_2 by employing a value for k_2 twice that shown in Table 1, but identical values for the ratios $k_3/k_2 = 10^{1.38}$ and $k_4/k_2 = 10^{-2.16}$.

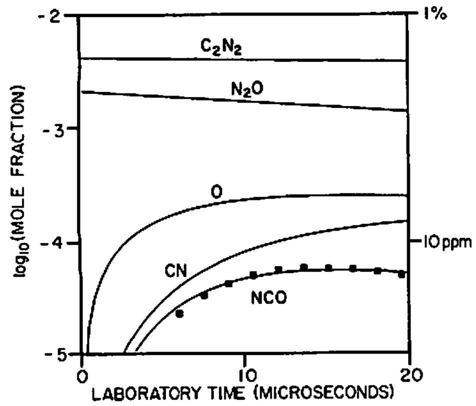

Fig. 4. Computer-generated profiles of C_2N_2, N_2O, O, CN, and NCO mole fractions using $k_3/k_2 = 10^{1.38}$ and $k_4/k_2 = 10^{-2.16}$ from Fig. 3, and the conditions of Fig. 2. The solid squares are taken from the NCO experimental trace of Fig. 2.

we assumed for k_4 an activation energy equal to the NCO dissociation energy, i.e., 47.3 kcal/mole [10], and a number of effective degrees of freedom $s = 2$ [11]. [The latter assumption implies a temperature exponent in the preexponential factor of k_4 equal to $m = 3/2 - s = -1/2$.] In addition, we assumed no temperature dependence for k_3 in the range $2150 \leqslant T \leqslant 2400$°K. Using a least-squares-fit expression based on the three experimental data points, we found $k_3/k_4 \simeq 10^{-3.1}T^{0.5} \exp[+24000/T]$ [$\times 2.0$, $\times 0.5$] for $2150 \leqslant T \leqslant 2400$°K.

No experimental measurement of k_3 has been performed above 1500°K. However, it is reasonable to assume that k_3 is nearly constant over a large temperature range. Using our earlier measurement of $k_3 = 10^{13.75}$ cm^3/mole/sec [$\times 1.60$, $\times 0.55$] at 1450°K [3] and combining the corresponding uncertainties in k_3 and k_3/k_4, we recommend $k_4 \simeq 10^{16.8}T^{-0.5} \exp[-24000/T]$ [$\times 2.3$, $\times 0.4$] over the range $2150 \leqslant T \leqslant 2400$°K. There are no previous data for k_4 available for comparison.

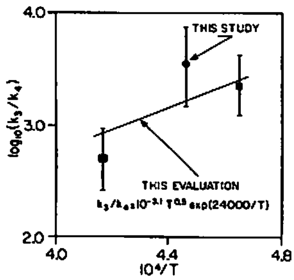

Fig. 5. Arrhenius plot for the ratio k_3/k_4. The square symbols are from Louge and Hanson [1]. Note that the corresponding experiments at $T = 2150$ and 2400°K were performed using independent NO and CN measurements [1].

$N_2O/O_2/H_2/C_2N_2/Ar$ MIXTURE—ANALYSIS AND RESULTS

The mechanism shown in Table 2 was used in the data reduction, but a simplified model based on the following reactions is helpful in understanding the influence of k_5 and k_6/k_7 on the measured NCO profile. As before, N_2O decomposes first to provide O-atoms. The influx of O-atoms is sufficient to trigger reactions in the O/H system that lead to partial equilibrium concentrations of H, O, and OH. Because of the relative proportions of O_2 and H_2 in the initial mixture, H is the dominant species in the O/H system [12] and reaction (6) becomes the major sink of C_2N_2:

$$C_2N_2 + H \rightarrow CN + HCN. \qquad (6)$$

The CN radicals formed by reaction (6) can in turn react with H_2 via reaction (7),

$$CN + H_2 \rightarrow HCN + H, \qquad (7)$$

or react with O_2 to form NCO via reaction (9),

$$CN + O_2 \rightarrow NCO + O. \qquad (9)$$

Finally, NCO is removed by H-atoms via reaction (5),

$$NCO + H \rightarrow NH + CO. \qquad (5)$$

For the purpose of this simplified mechanism, we can assume that CN has reached steady-state (ss) between reactions (6) and (7), and hence

$$\frac{[CN]^{ss}}{[C_2N_2]} \simeq \frac{k_6}{k_7} \times \frac{[H]^{pe}}{[H_2]} .$$

(pe = partial equilibrium). Further, the rate of

TABLE 2
Reaction Mechanism—$N_2O/O_2/H_2/C_2N_2/Ar$ Mixture

	Reaction	ΔH^a	Equilibrium Constant[b]	Rate Constant[c]			Reference
				$\log_{10} A$	m	$\theta(°K)$	
1	$N_2O + M \rightarrow N_2 + O + M$	+40	−3.8	23.89	−2.5	32,710	[16]
2	$C_2N_2 + O \rightarrow CN + NCO$	+4	0.3	12.66	0	4440	[1]
3	$NCO + O \rightarrow NO + CO$	−105	15.4	13.75	0	0	[3]
4	$NCO + M \rightarrow N + CO + M$	+48	−5.8	16.80	−0.5	24,000	This study
5	$NCO + H \rightarrow CO + NH$	−39	6.0	14.02	0	1000	This study[d]
6	$C_2N_2 + H \rightarrow CN + HCN$	+4	0.7	14.50	0	4030	This study
7	$CN + H_2 \rightarrow HCN + H$	−16	1.8	11.74	0.7	2460	[13]
8	$NCO + H_2 \rightarrow (HNCO) + H$	−10	1.0	13.23	0	4000	This study[e]
9	$CN + O_2 \rightarrow NCO + O$	−2	0.1	12.75	0	0	[1]
10	$CN + O \rightarrow CO + N$	−75	10.2	13.31	0	210	[1]
11	$N_2O + O \rightarrow NO + NO$	−38	7.1	13.84	0	13,400	[16]
12	$N_2O + O \rightarrow N_2 + O_2$	−81	12.1	14.00	0	14,100	[16]
13	$N_2 + O \rightarrow N + NO$	+75	−10.3	14.26	0	38,370	[16]
14	$NO + O \rightarrow N + O_2$	+32	−5.3	9.58	1.0	20,820	[16]
15	$NCO + N \rightarrow N_2 + CO$	−180	25.7	13.30	0	0	[18]
16	$NCO + N \rightarrow CN + NO$	−30	5.2	14.66	0	5530	[19][f]
17	$N_2O + H \rightarrow N_2 + OH$	−65	10.8	13.88	0	7600	[16]
18	$NH + NO \rightarrow N_2O + H$	−28	2.3	12.03	0	230	[16]
19	$NO + H \rightarrow N + OH$	+48	−6.6	14.23	0	24,560	[16]
20	$O_2 + H \rightarrow OH + O$	+16	−1.2	17.57	−1.0	8810	[22]
21	$H_2 + O \rightarrow H + OH$	+2	+0.1	10.26	1.0	4480	[22]
22	$H_2O + O \rightarrow OH + OH$	+17	−1.5	9.66	1.3	8605	[22]
23	$OH + H_2 \rightarrow H + H_2O$	−15	1.6	9.07	1.3	1825	[23]
24	$HCN + O \rightarrow NCO + H$	0	−0.4	8.24	1.47	3775	[3]
25	$HCN + O \rightarrow NH + CO$	−39	5.6	8.73	1.2	3820	[24]
26	$HCN + OH \rightarrow H_2O + CN$	+1	−0.2	12.64	0	4530	[13]
27	$CN + OH \rightarrow NCO + H$	−18	1.4	13.75	0	0	[25]
28	$C_2N_2 + OH \rightarrow HNCO + CN$	−8	1.3	11.27	0	1450	[26][g]
29	$HNCO + H \rightarrow NH_2 + CO$	−17	2.8	14.00	0	4280	[28]
30	$NH + H \rightarrow N + H_2$	−20	2.7	13.70	0	1000	[16]
31	$NH_2 + H \rightarrow NH + H_2$	−11	2.2	13.28	0	0	[16]

[a] Heat of reaction at 1500°K (kcal/mole) [10]; we used $\Delta Hf_0°(CN) = 101.2$ kcal/mole [10, 27].

[b] $\log_{10}(k_{forward}/k_{backward})$ at 1500°K [10].

[c] Using the notation $k = AT^m/\exp[\theta/T]$ (cm^3/mole/s).

[d] We estimated an activation energy of 2 kcal/mole for this reaction.

[e] We estimated an activation energy of 8 kcal/mole for this reaction. The form of the product (HNCO) is uncertain.

[f] Colket measured $k_{backward} = 10^{14} \exp[-21190/T]$ (cm^3/mole/s); we assumed $k_f/k_b = 4.54 \exp[15660/T]$.

[g] The products of this slow reaction are uncertain.

change of NCO concentration is given by

$$\frac{d[NCO]}{dt} \simeq k_9[CN][O_2] - k_5[NCO][H].$$

If C_2N_2, O_2, and H_2 are nearly constant throughout the period of interest, the NCO profile peaks at a value ($d[NCO]/dt = 0$) where, after substituting the above relations for $[CN]_{ss}$, we obtain

$$\frac{[NCO]^{peak}}{[C_2N_2]} \simeq \frac{k_9}{k_5} \times \frac{k_6}{k_7} \times \frac{[O_2]}{[H_2]}.$$

For this simplified model, the relative NCO profile (using the peak as a reference) depends primarily on the rate of reaction (5), since (after substituting the relation for $[CN]_{ss}$ in the NCO rate equation)

$$\frac{d[NCO]/[NCO]^{peak}}{dt} \simeq k_5[H][1 - [NCO]/[NCO]^{peak}].$$

The NCO peak concentration thus depends primarily on $(k_9/k_5) \times (k_6/k_7)$ and the relative time behavior depends on k_5. A record of NCO is therefore sufficient to infer k_5; using the established value of k_9 [1] and the measured NCO peak concentration [2], the ratio k_6/k_7 can also be inferred.

Despite the apparent simplicity of this model, we found it necessary to use a computer fitting technique to explain further the influence of key rate parameters on the NCO profile. In particular, we found that, despite the small value of k_8, the experimental time histories cannot be adequately fitted without accounting for reaction (8),

$$NCO + H_2 \rightarrow HNCO + H, \qquad (8)$$

because of the large quantities of H_2 present in the mixture. We assumed that the products of reaction (8) are HNCO + H ($\Delta H \simeq -10$ kcal/mole at 1500°K), rather than the thermodynamically favored NH_2 + CO ($\Delta H \simeq -27$ kcal/mole at 1500°K), because the path to NH_2 + CO requires a complex rearrangement of the molecular bonds. Using computer calculations based on the mechanism of Table 2, we identified three features of the NCO profile which could be simultaneously fitted to yield the three rate parameters of interest, namely k_5, k_6/k_7, and k_8. These three features are the absolute peak NCO concentration, the relative initial slope, and the relative decay of the NCO profile (using the peak as a reference). Figure 6 shows a best computer fit to the experimental trace. The computed effects of variations in k_5, k_6/k_7 and k_8 on the three features are illustrated in Table 3. For example, this table shows that an increase (↑) in k_6/k_7 would result in increases (↑) in relative initial slope and absolute peak concentration, and to a faster relative decay of the NCO profile.

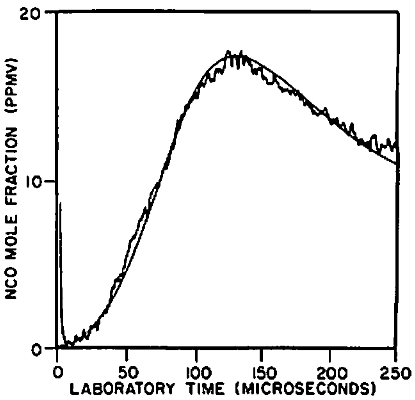

Fig. 6. Experimental trace with T_2 = 1490°K, p_2 = 0.63 atm, $N_2O : O_2 : H_2 : C_2N_2 : Ar = 4 : 1 : 6 : 4 : 985$ *and* ρ_{21} = 3.34. The peak absorption of 3.3% corresponds to χ_{NCO} = 17 ppmv with $\beta \simeq 103$ cm^{-1} atm^{-1} [2]. The solid line is a best computer fit to the data using $k_5 = 10^{13.73}$ cm^3/mole/s, $k_6/k_7 = 0.81$, $k_8 = 10^{12.1}$ cm^3/mole/s, and other rates in Table 2.

Figure 7 illustrates the effect of k_6/k_7 on the relative NCO profile. Note from Table 3 that k_5 and k_8 both have similar effects (↓) on the absolute peak concentration, but opposite effects on the relative initial slope; further, k_5 and k_8 do not substantially influence the relative decay. It therefore appears possbile to determine k_5, k_6/k_7, and k_8 by fitting the NCO trace alone. A unique value for k_6/k_7 can fit the relative

TABLE 3

NCO Profile Sensitivity[a]

	Characteristic Features		
Rates	Relative Slope	Peak Concentration	Relative Decay
k_5 ↑ (×2)	↑	↓ (×0.64)	↔
(k_6/k_7) ↑ (×2)	↑	↑ (×1.42)	↑
k_8 ↑ (×2)	↓	↓ (×0.82)	↔

[a] Legend: ↑, increasing value; ↓, decreasing value; ↔, no variation.

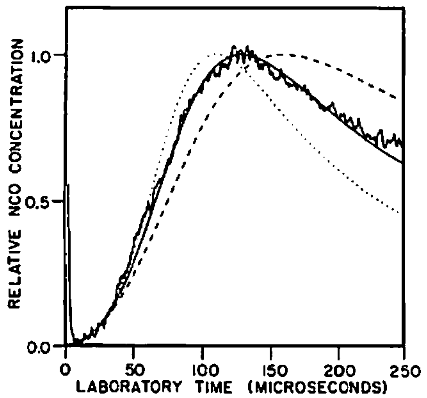

Fig. 7. Effect of the ratio k_6/k_7 on the relative NCO time history. The dotted line corresponds to $(k_6/k_7) \times 2.0$ and the dashed line to $(k_6/k_7) \times 0.5$.

decay, and a unique set of values for k_5 and k_8 can simultaneously fit the relative initial slope and the absolute peak concentration. Figure 8 illustrates the effect of k_5 on the relative NCO profile.

On the basis of this analysis, we found $k_5 = 10^{13.73(+0.42,-0.27)}$ cm²/mole/s, $k_6/k_7 = 0.81$ (+0.89, −0.47) and $k_8 = 10^{12.1(+0.4,-0.7)}$ cm³/mole/s. Uncertainties in k_5 result from the uncertain knowledge of other reactions in the mechanism [×1.7, ×0.57] and the uncertainty in the measured NCO peak concentration resulting in uncertainty factors in k_5 of [×2.1, ×0.75] [2]. Uncertainties in k_6/k_7 are attributed primarily to the uncertain knowledge of other rates [×2.1, ×0.42], because no absolute knowledge of the NCO concentration was required to fit the relative decay slope to k_6/k_7. Uncertainties in k_8 are fairly large [×2.5, ×0.2] and can be attributed mostly to the uncertainty in the absolute peak NCO concentration. A significant reduction in the overall uncertainty of k_5 and k_8 could be achieved if a more precise value of β(1490°K) were available. No significant uncertainty resulted from uncertain heats of formation (e.g., for CN, NCO, or NH) since most reactions proceeded in the forward direction.

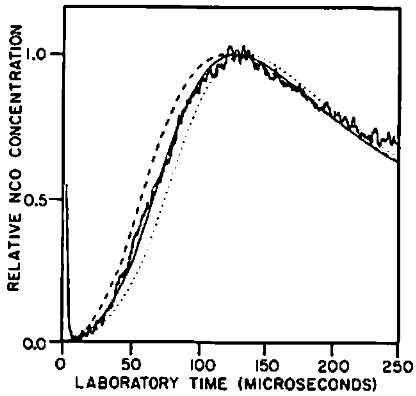

Fig. 8. Effect of k_5 on the relative NCO time history. The dotted line corresponds to $k_5 \times 0.5$ and the dashed line to k_5 × 2.0.

There are no previous data of k_5 and k_8 available for comparison. Miller et al. [13] recently calculated an expression for k_7 based on the measurements of Szekely et al. [5] in the range $2700 \leqslant T \leqslant 3500$°K and Albers et al. [14] at lower temperatures: $k_7 = 10^{11.74}T^{0.7}$ $\exp[-2460/T]$ cm³/mole/s. Judging from the error bars attached to the high and low temperature data, we believe the above expression should be valid within a factor of two at 1490°K. By using our measurement of k_6/k_7, this expression leads to $k_6 = 10^{13.15(\pm 0.5)}$ cm³/mole/s at 1490°K. Another estimate of k_6 can be obtained from the reverse rate k_{-6} measured by Szekely et al. [6] at high temperatures, with the result $k_6 = 10^{14.1(\pm 0.5)}$ cm³/mole/s at the average temperature of 2900°K [15]. Figure 9 is an Arrhenius plot of k_6. By using the two values of k_6 at 2900 and 1490°K, a straight Arrhenius fit would lead to $k_6 = 10^{15.1}$ $\exp[-6700/T]$ cm³/mole/s. However, the corresponding activation energy and preexponential factor of the fit

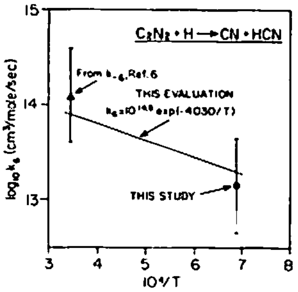

Fig. 9. Arrhenius plot for k_6.

appear too high for this mildly endothermic reaction ($\Delta H_R < 5.3$ kcal/mole at 2000°K [10, 27]). A more realistic activation energy of 8 kcal/mole leads to the expression $k_6 = 10^{14.5} \exp[-4030/T]$ cm^3/mole/s, which we recommend within factors of [$\times 3.2$, $\times 0.32$] over the range $1490 \leqslant T \leqslant 3070$°K.

This work was supported by the Air Force Office of Scientific Research under Contract No. F 49620-83K-0004 and the Environmental Protection Agency under Contract No. R-810019. Useful conversations with A. Szekely of this laboratory are gratefully acknowledged.

REFERENCES

1. Louge, M. Y., and Hanson, R. K., *Int. J. Chem. Kinet.*, 16:231 (1984).
2. Louge, M. Y., Hanson, R. K., Rea, E. C., and Booman, R. A., *J. Quant. Spectrosc. Radiat. Transfer*, in press.
3. Louge, M. Y., and Hanson, R. K., accepted for presentation at the *20th Symposium (International) on Combustion*, University of Michigan, August 1984.
4. Baulch, D. L., Duxbury, J., Grant, S. J., and Montague, D. C., *J. of Phys. Chem. Ref. Data* 10 (Suppl. 1):1-576 (1981).
5. Szekely, A., Hanson, R. K., and Bowman, C. T., *Int. J. Chem. Kinet.* 15:915 (1983).
6. Szekely, A., Hanson, R. K., and Bowman, C. T., *Int. J. Chem. Kinet.* 15:1237 (1983).
7. Monat, J. P., Hanson, R. K., and Kruger, C. H., *Comb. Sci. Tech.* 16:21 (1977).
8. Bittker, D. A., and Scullin, V. J., NASA TN D-6586, 1972.
9. Bowker, A. H., Lieberman, G. J., *Engineering Statistics*, 2nd ed., Prentice-Hall, Englewood Cliffs, NJ, 1972.
10. *JANAF Thermochemical Tables* (D. R. Stull and H. Prophet, Project Directors), Natl. Bur. Stand., Washington D.C., NBS 37, 2nd ed., 1971.
11. Vincenti, W. G., and Kruger, C. H., *Introduction to Physical Gas Dynamics*, R. E. Krieger, Huntington, NY, 1977, p. 223.
12. Dove, J. E., and Nip, W. S., *Can. J. Chem.* 52:1171 (1974).
13. Miller, J. A., Branch, M. C., McLean, W. J., Chandler, D. W., Smooke, M. D., and Kee, R. J., accepted for presentation at the *20th Symposium (International) on Combustion*, University of Michigan, August 1984.
14. Albers, E. A., Hoyermann, K., Schacke, H., Schmatjko, K. J., Wagner, H. Gg., and Wolfrum, J., *Proceedings of the 15th Symposium (International) on Combustion, 1974*, The Combustion Institute, Pittsburgh, 1975, p. 765.
15. Szekely, A., Ph.D. Thesis, Stanford University, 1984.
16. Hanson, R. K., and Salimian, S., in *Survey of Rate Constants in the N/H/O System* (W. Gardiner, Ed.), Springer Verlag, in press.
17. Fueno, T., Tabayashi, K., and Kajimoto, O., *J. Phys. Chem.* 77:575 (1973).
18. Lifshitz, A., and Frenklach, M., *Int. J. Chem. Kinet.* 12:159 (1980).
19. Colket, M. B., *Int. J. Chem. Kinet.* 16:353 (1984).
20. Slack, M. W., *J. Chem. Phys.* 64:228 (1976).
21. Unpublished estimates based on transition state theory and best fits of CN records in experiments at 1600°K, 1 atm with $N_2O : C_2N_2 : Ar = 25 : 4 : 971$.
22. Cohen, N., and Westberg, K. R., Aerospace Corporation, ATR-82 (7888)-3, 1982.
23. Dixon-Lewis, G., and Williams, D. J., *Comprehensive Chemical Kinetics*, vol. 17 (1) (C. H. Bamford and C. F. H. Tipper, Eds.), Elsevier, Amsterdam.
24. Perry, R. A., and Melius, C. F., accepted for presentation in the *20th Symposium (International) on Combustion*, University of Michigan, August 1984.
25. Haynes, B. S., *Combust. Flame* 28:113 (1977).
26. Phillips, L. F., *Combust. Flame* 35:233 (1979).
27. Colket, M. B., *J. Quant. Spectrosc. Radiat. Transfer* 31:7 (1984).
28. Peterson, R. C., Ph.D. Thesis, Purdue University 1981.

Received 17 April 1984; revised 28 June 1984